Particle Filters for Hybrid Event Sensor Fusion with 3D Vision and Force.

Wim Meeussen, Johan Rutgeerts, Klaas Gadeyne, Herman Bruyninckx, Joris De Schutter
Department of Mechanical Engineering, Katholieke Universiteit Leuven,
Celestijnenlaan 300B, B-3001 Leuven, Belgium.
Email: wim.meeussen@mech.kuleuven.be

***Abstract*— This paper presents a contribution to Bayesian based sensor fusing in the context of human demonstration for compliant motion task specification, where sensor-controlled robot systems physically interact with the environment. One wants to learn about the geometric parameters of a task and segment the total motion executed during the human demonstration into subtasks for the robot. The motion of the human demonstration tool is sensed by measuring the position of multiple LED markers with a 3D camera, and the interaction with the environment is sensed with a force/torque sensor inside the demonstration tool. All measurements are uncertain, and do not give direct information about the *geometric* parameters of the contacting surfaces, or about the *contact formations* encountered during the human demonstration. The paper uses a Bayesian Sequential Monte Carlo method (also known as a *particle filter*) to simultaneously estimate the contact formation (discrete information) and the geometric parameters (continuous information), where different measurement models link the information from heterogeneous sensors to the hybrid unknown parameters. The simultaneous contact formation segmentation and the geometric parameter estimation are helped by the availability of a *contact state graph* of all possible contact formations. The presented approach applies to all compliant motion tasks involving polyhedral objects with a known geometry, where the uncertain geometric parameters are the poses of the objects. The approach has been verified in real world experiments, in which it is able to discriminate in realtime between some 250 different contact formations in the graph.**

I. Introduction

Compliant motion [1] refers to tasks in which an object held by a manipulator moves while maintaining contact with the environment. The force interaction at the contact is used to guide the manipulated object along the surface of the environmental object, to help overcome geometric uncertainties associated with the task, or to help overcome the limited absolute accuracy of a manipulator. Major challenges for the planning and execution of compliant motion tasks are: (i) to recognize the *contact formation* to which the contacting objects are subjected, (ii) to estimate the geometric parameters of that contact formation (i.e., position of contact point(s), direction of contact normal(s), etc.), and (iii) to detect when exactly the changes between two contact formations occur. However, even between two simple polyhedral objects, *hundreds* of contact formations are possible, and, hence, hundreds of transitions between contact formations.

Initial research on the identification of contact formations mainly focused on two different approaches: (i) ad hoc identification strategies that exploit geometric knowledge of the contacting objects, but that have a very poor stochastic foundation (e.g. [2]) and (ii) Hidden Markov Model based (hence stochastic) solutions to assembly problems that can recognize contact formation transitions very fast but only with limited allowed uncertainty (e.g. [3]). Most approaches only use information from one sensor, mostly a force sensor. Previous work by the research group of the authors has pioneered (in the domain of force-controlled compliant motion) the integration of both approaches, in combination with sensor information from multiple sensors. This *hybrid state space* estimation problem (also called "data association") involves *continuous* geometric parameters, that get their precise meaning only in the context of a *discrete* contact formation. The contact formation indicates the *model* that links the sensor data to the continuous state parameters. Using state-of-the-art Bayesian probability techniques, the information from various sensors (e.q. force sensor, camera, encoders, ...) is combined to simultaneously estimate contact formations and geometrical parameters related to the compliant motion task.

Fig. 1. In the experiment to validate the presented approach a cube is manipulated in contact with three perpendicular faces.

This paper focusses on hybrid event sensor fusing in compliant motion tasks. During the *human demonstration* of a compliant motion task, sensor data about the task is gathered by heterogeneous sensors mounted onto a demonstration tool that is used to manipulate the objects involved in the task. The sensor information consists of the contact forces and torques, and the position in space of multiple LED markers mounted onto the demonstration tool. After the demonstration, in an interpretation step, the sensor data is used in the measurement models of a *particle filter*

[4] to recognize, simultaneously, discrete contact transitions, and estimate continuous geometric parameters. The presented approach is able to estimate a 12-dimensional geometric parameter, and simultaneously recognize contact transitions in an experiment consisting of as many as 245 possible contact formations. The efficiency of the algorithm that implement the measurement models allows us to use the particle filters in *realtime*.

The paper is organized as follows. Section II briefly reviews the concepts of contact formations and the contact state graph. Section III describes the demonstration tool which is used to collect sensor data during human demonstration in compliant motion. The interpretation of this sensor data, using Bayesian estimation techniques, is covered in Section IV, while Section V describes the real world experiments that validate the presented approach. Finally, Section VI contains conclusions and future work.

II. Contact Formations and the Contact State Graph

A. Contact Formations

The notion of *principal contacts* (PCs) was introduced [5] to describe a contact primitive between two surface elements of two polyhedral objects in contact, where a surface element can be a face, an edge or a vertex. The *boundary elements* of a face are the edges and vertices bounding it, and the boundary elements of an edge are the vertices bounding it. Formally, a PC denotes the contact between a pair of surface elements which are not boundary elements of other contacting surface elements. Fig. 2 shows the six non-degenerate PCs that can be formed between two polyhedral objects. Each non-degenerate PC is associated with a *contact plane*, defined by a contacting face or the two contacting edges at an edge-edge PC.

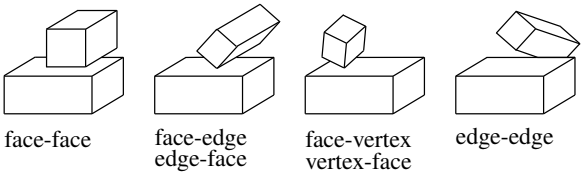

Fig. 2. The six possible non-degenerate principal contacts (PCs) between two polyhedral objects.

A general contact state between two objects can be characterized topologically by the set of PCs formed, called a *contact formation* (CF). Each configuration of two objects, i.e. their relative pose in space, compliant to the constraints of a CF, is called a *CF-compliant configuration*, denoted by a pose $\boldsymbol{X}$. Any motion formed by a sequence of CF-compliant configurations is called a *CF-compliant motion*.

A PC can be decomposed into one or more *Elementary Contacts* (ECs), providing a lower level description of the CF. The three types of ECs (face-vertex, vertex-face and edge-edge) are shown in the two examples at the right of Fig. 2. An EC is a point contact and is associated with a *contact point* and a *contact normal*.

B. Contact State Graph

Xiao and Ji developed a divide-and-merge approach [6], [7] to generate a compact, simplified representation of the contact state space between two polyhedral objects, as a *contact state graph* G. In G a node represents a CF, and an arc connecting two nodes represents the adjacency relationship between the CFs of the nodes. Two CFs CF_i and CF_j are adjacent if a compliant motion from a CF_i-compliant configuration to CF_j-compliant configuration exists, which only includes CF_i and CF_j-compliant configurations. Fig. 3 shows an example of a contact state graph containing seven different CFs and their adjacency relationships. The approach was implemented to automatically generate a contact state graph that can contain hundreds of contact formations.

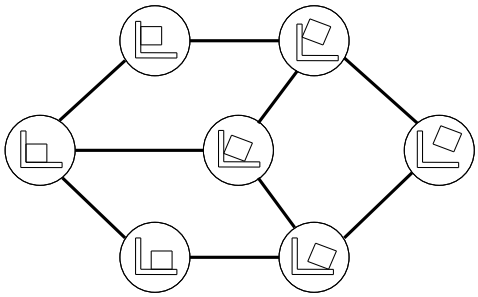

Fig. 3. A complete contact state graph shows all possible CFs (nodes) and transitions between neighboring CFs (arcs). While this figure shows a simplified example that only contains 7 CFs, a real contact state graph of two 3-dimensional polyhedral objects contains hundreds of CFs.

III. Demonstration Tool

In programing by human demonstration, a task specification for a compliant task involving a manipulated object and its environment is obtained by observing a human demonstrate the desired task. In this research the human demonstrator directly interacts with the manipulated object, using a *demonstration tool* which is mounted onto the manipulated object.

A. Design

A model of the tool's design is shown in Fig. 4, while Fig. 1 shows the tool during an experiment. A handle on top provides an easy grasp for the human demonstrator to manipulate the demonstration tool and the object attached to it. The demonstration tool consists of nine faces, and up to four LED markers can be mounted on each face. The Krypton K600 6D optical system (Fig. 4) measures the spatial positions of the LED markers, at 100 $[Hz]$, with a volumetric accuracy of 90 $[\mu m]$. Inside the demonstration tool, a *JR3* wrench sensor is mounted between the demonstration tool and the manipulated object, to measure the wrench $\boldsymbol{w}_m$ (linear force and moment) applied by the human demonstrator to the manipulated object. The calibration of the demonstration tool is discussed in [8].

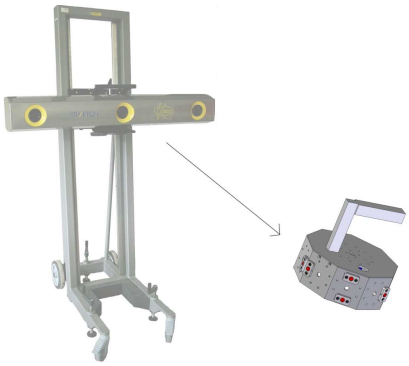

Fig. 4. The Krypton K600 6D optical system uses three cameras and triangulation algorithms to accurately measure the spacial position of each of the LED markers on the demonstration tool.

B. Kalman filter to merge position measurements of the LED markers

While the wrench $\boldsymbol{w}_m$ is directly measured by a physical sensor, the pose $\boldsymbol{X}_m$ (position and orientation) and twist $\boldsymbol{t}_m$ (translational and rotational velocity) between the contacting objects are indirectly measured through the positions of the LED markers that are visible to all three camera's. Due to the geometry of the demonstration tool, the maximum number of simultaneously visible LED markers is 12, while at least 4 visible LED markers are needed by our algorithm to extract the pose and twist of the demonstration tool.

Say the number of LED markers visible to all three camera's is $v \geq 4$. Then the camera system measures v positions $\boldsymbol{p}_1^c \ldots \boldsymbol{p}_v^c$, relative to the camera (c). The positions of the LED markers $\boldsymbol{p}_1^d \ldots \boldsymbol{p}_v^d$ relative to the demonstration tool (d), are known from an initial calibration phase. In a first step, the pose matrix (rotation matrix $\boldsymbol{R}_c^d$ and position vector $\boldsymbol{p}_c^d$) of the demonstration tool is calculated in a minimization problem:

$$\begin{bmatrix} \boldsymbol{R}_c^d & \boldsymbol{p}_c^d \end{bmatrix} = \begin{bmatrix} \boldsymbol{p}_1^c & \ldots & \boldsymbol{p}_v^c \end{bmatrix} \begin{bmatrix} \boldsymbol{p}_1^d & \ldots & \boldsymbol{p}_v^d \\ 1 & \ldots & 1 \end{bmatrix}^{\dagger}, \quad (1)$$

in which † represents the pseudo-inverse of a matrix.

In a second step, this calculated pose is an input to a linear estimation problem to obtain both the demonstration tool's pose $\boldsymbol{X}_m$ and twist $\boldsymbol{t}_m$, based on a constant acceleration model [9]. The Kalman filter is the preferred tool for this linear estimation problem with low uncertainties. The filter uses an 18-dimensional state vector which contains the pose vector $\boldsymbol{x}$ (XYZ position and ZYX Euler angles), the velocity $\dot{\boldsymbol{x}}$ and the acceleration $\ddot{\boldsymbol{x}}$. All three 6-dimensional parameters are estimated from the initially calculated pose. The filter's system model extrapolates the estimated pose $\hat{\boldsymbol{x}}$, velocity $\hat{\dot{\boldsymbol{x}}}$ and acceleration $\hat{\ddot{\boldsymbol{x}}}$ at time step k, to make a prediction of the pose $\tilde{\boldsymbol{x}}$, velocity $\tilde{\dot{\boldsymbol{x}}}$ and acceleration $\tilde{\ddot{\boldsymbol{x}}}$ at time step $k+1$, using a constant acceleration model. Then, the filter's measurement model uses the difference between the calculated pose from the previous minimization problem and the predicted pose $\tilde{\boldsymbol{x}}$ at time step $k+1$, to update the estimated pose $\hat{\boldsymbol{x}}$, velocity $\hat{\dot{\boldsymbol{x}}}$ and acceleration $\hat{\ddot{\boldsymbol{x}}}$ at time step $k+1$. This results in an estimated pose vector $\hat{\boldsymbol{x}}$ and a velocity vector $\hat{\dot{\boldsymbol{x}}}$, which are converted into a pose $\boldsymbol{X}_m$ and a twist $\boldsymbol{t}_m$.

IV. Simultaneous Recognition of Contact Formations and Estimation of Geometric Parameters

This section shows how the measurements of the $\boldsymbol{w}_m$, the twist $\boldsymbol{t}_m$ and the pose $\boldsymbol{X}_m$ are combined to segment a compliant motion task into a sequence of CFs, and simultaneously estimate geometrical parameters. At each CF, different contact constraints apply. Therefore, to estimate uncertain geometric parameters of the objects involved in a compliant motion task, the knowledge of the current CF model is required. This means that the estimation problem for compliant motion tasks, consists of a hybrid problem: the recognition of the (discrete) CF and the estimation of (continuous) geometric parameters.

In this paper particle filters [4] are used to implement this hybrid estimation problem. Gadeyne et al. [10] show that while Kalman filter variants cannot cope with the cross-dependency between discrete and continuous variables, using a hybrid PDF, particle filters can. The particle filter algorithm updates the discrete CF and continuous geometric parameters in two steps. In the first step the system model makes a prediction for the next CF and the geometric parameters. In the second step the measurement model corrects this prediction based on sensor data from different sensors. This section describes the models that are used in the estimation problem.

A. Hybrid Probability Density Function

The 13-dimensional hybrid *probability density function* (PDF) in the studied compliant motion task contains a 12-dimensional continuous parameter and one discrete state. The continuous parameter represents the unknown pose of the environmental object relative to a world reference, and the unknown pose of the manipulated object relative to the demonstration tool. Note that while the pose of the objects is unknown, their geometry is known. The discrete state contains the CF between the manipulated object and the environment, and can be any of the many hundreds of CFs in a complete contact state graph of the contacting objects.

B. System Model – Prediction

The system update calculates the prediction density at time step k, given the estimated variables at time step $k-1$. This prediction step is based on the probability of a transition from a CF i at time step $k-1$ to a CF j at time step k. To predict the next CF out of hundreds of theoretically possible next CFs, the topological information from the objects' contact state graph is used. Between two adjacent CFs in the contact state graph, a direct transition is possible, while between two not-adjacent CFs a transition is only possible through one or more other CFs. This topological information drastically reduces the number of possible next CFs. If two CFs i and j are not adjacent, the probability of a transition is zero. For

two adjacent CFs i and j, the probability of a transition is defined by the distance vector $\boldsymbol{d}_m$ between the two objects, which is explained in detail in the next subsection. The closer the two objects are, the more likely a transition will occur.

C. Measurement Model – Correction

The correction step uses measurement models to calculate the hybrid joint density at time step k, given the prediction for the hybrid joint density at time step k. A measurement model represents the belief in a sensor measurement, given the geometric parameters and the CF. In this research we combine the sensor information from heterogeneous sensors with two different measurement models. The first model is based on the pose measurement $\boldsymbol{X}_m$, and the second model is based on the wrench and twist measurements $\boldsymbol{w}_m$ and $\boldsymbol{t}_m$. Both measurements models are applied in every correction step.

1) Contact distance measurement model based on pose measurements: The decomposition of a general CF into ECs (Section II) allows the automatic generation of the contact distance measurement equation for different CF models. Say the number of possible ECs between the manipulated object and the environmental object at *all possible* CFs is p. Each CF in the contact state graph can be decomposed into one or more ECs, therefore, the total number of possible ECs is ever greater than the number of CFs, and typically in the range of 10^2 to 10^3. At each $EC_1 \dots EC_p$ the distance between the objects is calculated. A new measurement variable $\boldsymbol{d}_m$ is created from the pose measurement $\boldsymbol{X}_m$, by combining all these distances into one distance vector:

$$\boldsymbol{d}_m = \begin{bmatrix} d_1 & \dots & d_p \end{bmatrix}^T. \tag{2}$$

The contact distance measurement equation expresses the belief in the distance vector, given the current CF and the geometric parameters. This expresses that when the manipulated object is in contact with the environmental object, the distance between the objects at the contact points should be zero, thereby closing the kinematic chain between the objects. The distance between the objects at non-contact points should be greater than zero, expressing that the objects do not penetrate nor contact.

To achieve an efficient algorithm for the pose measurement model, the following three assumptions are made: (i) The probabilities on the distances $d_1 \dots d_p$ are assumed to be independent, although they are all linked to the probability of the measured pose $\boldsymbol{X}_m$. The probability of the distance vector is calculated as the product of the probabilities on the single distances. (ii) Not all the distances for at the ECs between the contacting objects are calculated; only the distances at ECs that are relevant in the currently assumed CF are calculated. The relevant distances are the distances at the ECs of the assumed CF, as well as the ECs directly connected to the assumed CF by an edge. (iii) The distance calculation at the ECs is helped by the use of spherical boundary boxes around the elements of the ECs. Only when two boundary boxes intersect, the exact distance at an EC is calculated. When the boundary boxes do not intersect (meaning that the elements of the EC are far apart) the exact distance has no real influence on the filter's behavior, and is approximated by the distance between the boundary boxes.

2) Residue measurement model based on wrench-twist measurements: The residue measurement model expresses the consistency between the contact constraints, and the wrench and twist measurements $\boldsymbol{w}_m$ and $\boldsymbol{t}_m$ [11], [12]. The consistency is expressed by a residue vector $\boldsymbol{r}_m$, which is the part of the measured twist and wrench that is not explained by the first order kinematics of an ideal frictionless contact; it should vanish when the measurements and the model are consistent. For a given pose and CF, the first order kinematics are represented by a wrench space $\boldsymbol{W}$ and a twist space $\boldsymbol{T}$. The wrench space contains all possible wrenches that can be applied between the contacting objects at the current pose, while the twist space contains all possible instantaneous twists that maintain the contact. The calculation of the wrench and twist space is discussed in [13]. The residue vector $\boldsymbol{r}_m$ is 12-dimensional and contains a six-dimensional wrench residue and a six-dimensional twist residue:

$$\boldsymbol{r}_m = \begin{bmatrix} \boldsymbol{I} - \boldsymbol{W}\boldsymbol{W}^{\dagger_{\boldsymbol{K}_w}} & \boldsymbol{0} \\ \boldsymbol{0} & \boldsymbol{I} - \boldsymbol{T}\boldsymbol{T}^{\dagger_{\boldsymbol{K}_t}} \end{bmatrix} \begin{bmatrix} \boldsymbol{w}_m \\ \boldsymbol{t}_m \end{bmatrix}. \tag{3}$$

The operator $^{\dagger_{\boldsymbol{K}_w}}$ represents the weighted pseudo-inverse [14] of a matrix using a weighting matrix $\boldsymbol{K}_w$. The residue is a nonlinear function of the pose $\boldsymbol{X}_m$, the CF, the geometrical parameters, and the measured wrench $\boldsymbol{w}_m$ and twist $\boldsymbol{t}_m$.

The calculation of the residue $\boldsymbol{r}_m$ includes one SVD for the calculation of the wrench and twist spaces, and two weighted pseudo-inverses $\boldsymbol{W}^{\dagger_{\boldsymbol{K}_w}}$ and $\boldsymbol{T}^{\dagger_{\boldsymbol{K}_t}}$ that each require another SVD. These calculations are numerically expensive. However, in [15] it is shown that when choosing the weighting matrices:

$$\boldsymbol{K}_t = \boldsymbol{K}_w^{-1}, \tag{4}$$

the numerical cost can be reduced to one single SVD by exploiting the orthonormal nature of the matrices calculated by the SVD algorithm. This reduces the computational cost of the overall filter with 55%.

The PDF of the residue $\boldsymbol{r}_m$ is represented by two 6-dimensional Gaussians, one for the wrench residue and one for the twist residue.

D. Implementation Details

The presented implementation is capable of processing $90,000$ particles[1] per second, on a 2 $[GHz]$ AMD 64 laptop, sufficient for realtime discrimination between 245 CFs and estimation of uncertain geometrical parameters. This performance is achieved by exploiting application-specific knowledge and using application-specific "shortcuts", such as:

- assuming probabilities to be independent,
- not calculating or only approximating probabilities that are not relevant,

[1]Processing one particle includes one system update, two measurement updates and the overhead of the particle filter such as re-sampling.

- developing numerically efficient algorithms, and
- choosing easy to evaluate PDFs.

The algorithms presented in this paper are implemented within the framework offered by the open source C++ Bayesian Filtering Library (BFL) [16]. BFL offers a unifying framework for all recursive Bayesian filters, such as Kalman filters, extended Kalman filters and particle filters. It provides efficient implementations of various filter algorithms.

The software for the automatic generation of a contact state graph, given a geometric description of two polyhedral objects, is provided by Jing Xiao of the University of North Carolina at Charlotte and her research group. Their algorithms generate a complete contact state graph containing hundreds of CFs, within seconds.

V. Experiments

This section reports on the real world experiment to validate the presented approach. In the experiment, a human demonstrator manipulates a cube through a complex sequence of CFs in an environment consisting of three perpendicular faces. Fig. 1 shows the experimental setup and Fig. 5 shows the sequence of CFs.

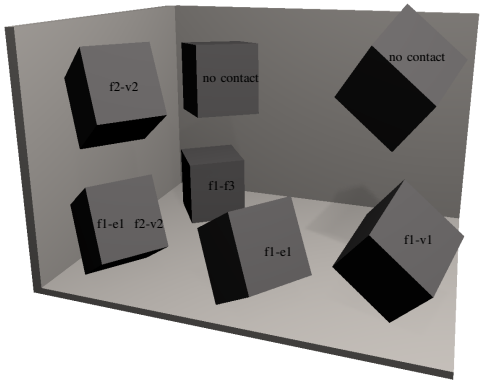

Fig. 5. The CF evolution of a human demonstration where a cube is manipulated in contact with two perpendicular faces.

A. Approach to First Contact

In the first part of the experiment, the cube has no contact with the environment, and approaches one of the planes of the environment. Fig. 6 shows the time evolution of the uncertainty on the z position of the environment. The uncertainty on this position is 1 component of the 12-dimensional continuous parameter; it is obtained by integrating over the 11 other components, for a given CF. The first five sub-figures show the position parameter for the no-contact CF, while the sixth sub-figure shows the position parameter for the first vertex-face CF. Initially the position is represented by a uniform distribution, indicating that there is little knowledge about its value. When the cube approaches the plane, the probability decreases on the left side of the distribution. This shows that the cube "penetrated" one of the possible positions of the plane without detecting a contact, thus proving that possible position invalid. This evolution continues until the cube makes a vertex-face CF with the plane. The CF transition is detected due to the inconsistency between the measured wrench and the assumed no-contact CF. The knowledge about the vertex-face CF allows accurate estimation of the position of the plane, also decreasing the probability on the right side of the uniform distribution.

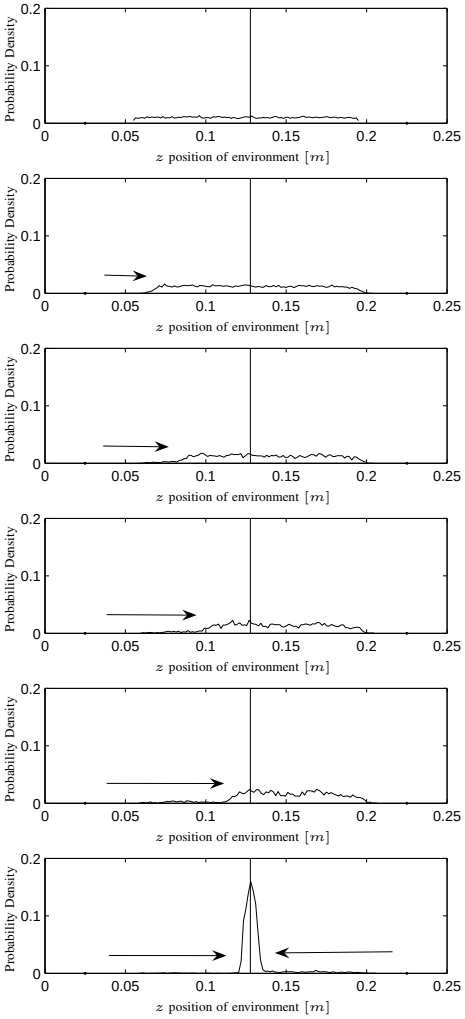

Fig. 6. The time evolution of the probability density on the position of a plane, when approaching the plane with a cube. The vertical line shows the true position of the plane. The probability density decreases gradually when the cube approaches. The last figure shows how the probability density suddenly decreases when the cube makes contact with the plane.

B. Sequence of Contact Formations

In the rest of the experiment, the cube is manipulated in contact with the environment, through a complex sequence of CFs. The demonstrated sequence of CFs and the dimension of the wrench and twist spaces is shown in Fig. 5.

The experiment includes complex CFs and CF transitions, such as adding contact constraints, removing contact constraints, adding many contact constraints at once, removing many contact constraints at once, and simultaneous contacts with the two planes. Fig. 7 shows the evolution of the estimated probability on each of the 245 possible CFs. Each CF is one possible value of the discrete state, and its probability is obtained by integrating over all 12 components of the continuous parameter, for each of the possible values of the discrete state. At each time step only a few CFs have a probability greater than zero. The particle filters successfully assign the highest probability to the CF that corresponds to the true CF in the experiment.

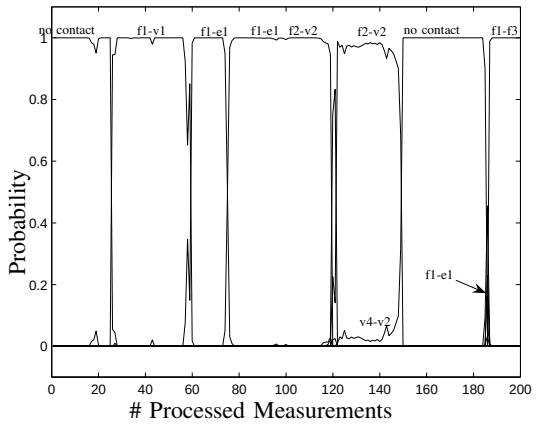

Fig. 7. The CF evolution of a human demonstration where a cube is manipulated in contact with two perpendicular faces. The evolution is shown by the probability on each of the CFs.

VI. Conclusions

This paper presents a contribution to sensor fusion in programming by human demonstration for sensor-controlled robot systems that physically interact with the environment, with a focus on compliant motion tasks. Sensor data from heterogeneous sensors is collected during a demonstration step. The krypton 6D optical 3-camera system measures the pose and twist of the manipulated object, while a wrench sensor measures the interaction forces and torques between the contacting objects. Subsequently, in an interpretation step, these measurements are mapped on a discrete CF and continuous geometrical parameters, using sequential Bayesian estimation techniques knows as particle filters.

Similar to the more familiar localization, tracking and recognition problems in mobile robotics, the approach *simultaneously* recognizes CF transitions and estimates geometrical parameters. The approach is based on particle filter which can cope with hybrid (partly discrete, partly continuous) joint posterior variables containing both the CF and geometrical parameters of the environment. While previously presented results in this field only allowed certain CFs or certain CF transitions, this approach scales the search space to *all possible CFs* between the contacting objects, using the topological information contained in a contact state graph. This extension in combination with new efficient algorithms, allow the *realtime* simultaneous recognition of CFs and estimation of geometric parameters. The approach applies to convex as well as to concave polyhedral objects with a known geometry, but at an unknown pose, and is able to efficiently recognize the CF at each step of a human demonstration out of many hundreds of possible CFs. Experimental results verify the effectiveness of the method.

Acknowledgment

All authors gratefully acknowledge the financial support by K.U.Leuven's Concerted Research Action GOA/05/10. The authors also acknowledge Jing Xiao of the university of North Carolina at Charlotte and her research group for providing their software for the automatic generation of a contact state graph.

References

[1] J. De Schutter and H. Van Brussel, "Compliant Motion I, II," *Int. J. Robotics Research*, vol. 7, no. 4, pp. 3–33, Aug 1988.

[2] A. O. Farahat, B. S. Graves, and J. C. Trinkle, "Identifying contact formations in the presence of uncertainty," in *Proc. IEEE/RSJ Int. Conf. Int. Robots and Systems*, Pittsburgh, PA, 1995.

[3] B. S. Eberman and J. K. Salisbury, Jr., "Application of change detection to dynamic contact sensing," *Int. J. Robotics Research*, vol. 13, no. 5, pp. 369–394, 1994.

[4] A. Doucet, N. J. Gordon, and V. Krishnamurthy, "Particle Filters for State Estimation of Jump Markov Linear Systems," *IEEE Trans. Signal Processing*, vol. 49, no. 3, pp. 613–624, march 2001.

[5] J. Xiao, "Automatic determination of topological contacts in the presence of sensing uncertainty," in *Int. Conf. Robotics and Automation*, Atlanta, GA, 1993, pp. 65–70.

[6] J. Xiao and X. Ji, "A Divide-And-Merge Approach to Automatic Generation of Contact States and Planning of Contact Motions," in *Int. Conf. Robotics and Automation*, San Francisco, CA, 2000, pp. 750–756.

[7] ——, "On automatic generation of high-level contact state space," *Int. J. Robotics Research*, vol. 20, no. 7, pp. 584–606, 2001.

[8] J. Rutgeerts, "A demonstration tool with Kalman Filter data processing for robot programming by human demonstration," in *Proc. IEEE/RSJ Int. Conf. Int. Robots and Systems*, Edmonton, Canada, 2005, pp. 3918–3923.

[9] Y. Bar-Shalom and X. Li, *Estimation and Tracking, Principles, Techniques, and Software*. Artech House, 1993.

[10] K. Gadeyne, T. Lefebvre, and H. Bruyninckx, "Bayesian hybrid model-state estimation applied to simultaneous contact formation recognition and geometrical parameter estimation," *Int. J. Robotics Research*, vol. 24, no. 8, pp. 615–630, 2005.

[11] H. Bruyninckx, J. De Schutter, and S. Dutré, "The "reciprocity" an "consistency" based approaches to uncertainty identification for compliant motions," in *Int. Conf. Robotics and Automation*, Atlanta, GA, 1993, pp. 349–354.

[12] M. S. Ohwovoriole and B. Roth, "An extension of screw theory," *Trans. ASME J. Mech. Design*, vol. 103, no. 4, pp. 725–735, 1981.

[13] W. Meeussen, J. De Schutter, H. Bruyninckx, J. Xiao, and E. Staffetti, "Integration of planning and execution in force controlled compliant motion," in *Proc. IEEE/RSJ Int. Conf. Int. Robots and Systems*, Edmonton, Canada, 2005, pp. 2550–2555.

[14] Y. Nakamura, *Advanced robotics: redundancy and optimization*. Reading, MA: Addison-Wesley, 1991.

[15] W. Meeussen, J. Rutgeerts, K. Gadeyne, H. Bruyninckx, and J. De Schutter, "Contact state segmentation using particle filters for programming by human demonstration in compliant motion tasks," K.U.Leuven, Leuven, Belgium, Tech. Rep., 2006.

[16] K. Gadeyne, "BFL: Bayesian Filtering Library," http://people.mech.kuleuven.ac.be/ kgadeyne/bfl, 2001.

[17] *Int. Conf. Robotics and Automation*, Atlanta, GA, 1993.

[18] *Proc. IEEE/RSJ Int. Conf. Int. Robots and Systems*, Edmonton, Canada, 2005.